

## Supporting Information

### A high-energy-density supercapacitor with multi-shelled nickel-manganese selenide hollow spheres as cathode and double-shell nickel-iron selenide hollow spheres as anode electrodes

Akbar Mohammadi Zardkhoshou\* Bahareh Ameri, and Saeid Saeed Hosseiny Davarani\*

Department of Chemistry, Shahid Beheshti University, G. C., 1983963113, Evin, Tehran, Iran.

Corresponding authors: \*Tel: +98 21 22431661; Fax: +98 21 22431661; E-mail: [ss-hosseiny@sbu.ac.ir](mailto:ss-hosseiny@sbu.ac.ir) (S.S.H. Davarani); and [mohammadi.bahadoran@gmail.com](mailto:mohammadi.bahadoran@gmail.com) (A. Mohammadi Zardkhoshou)

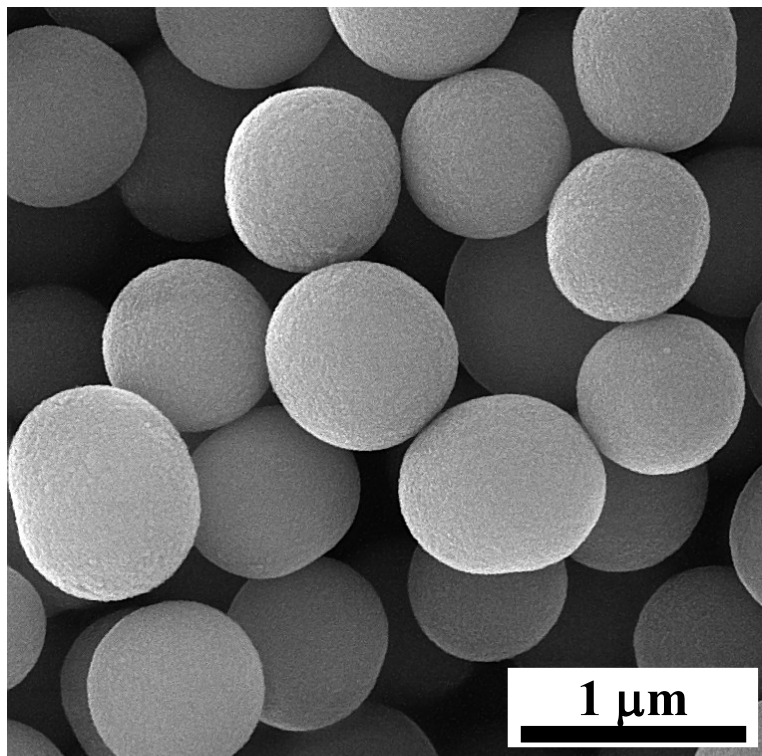


**Fig. S1.** FE-SEM image of the metal acetate-polysaccharides (MAPs).

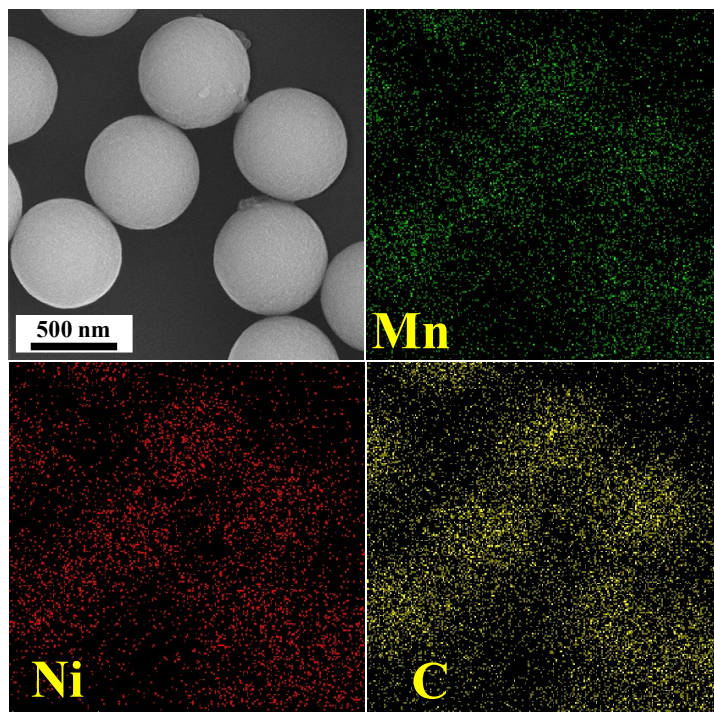


**Fig. S2.** EDS mapping of the metal acetate-polysaccharides (MAPs).

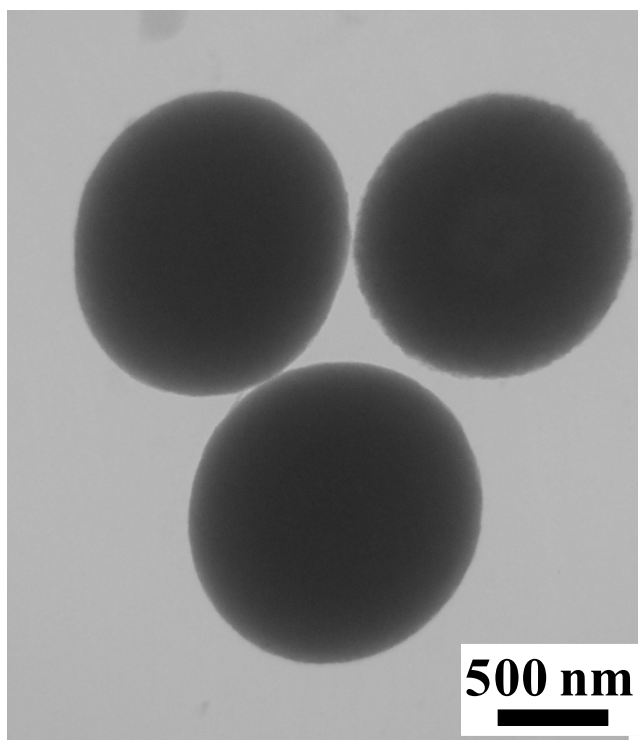


**Fig. S3.** TEM image of the metal acetate-polysaccharides (MAPs).

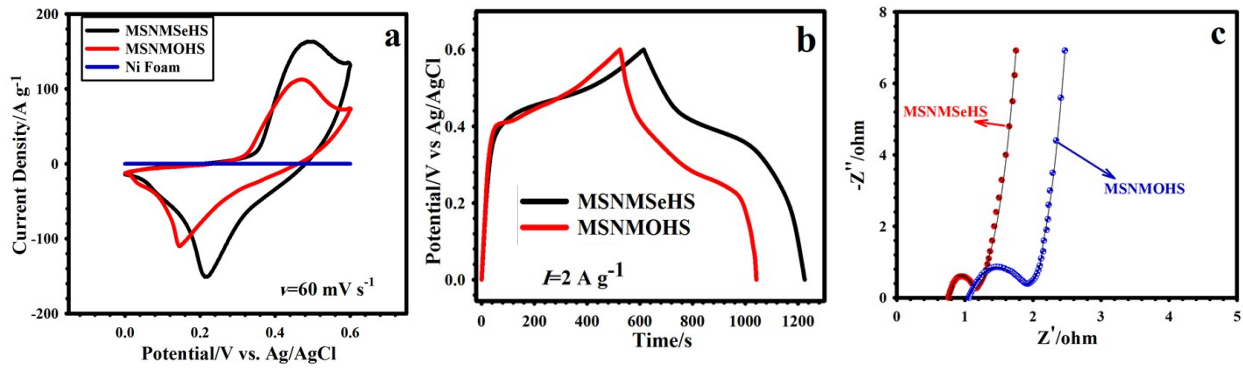


**Fig. S4.** (a) CV curves of the MSNMSeHS, MSNMOHS, and pure nickel foam at scan rate of  $60 \text{ mV s}^{-1}$ . (b) GCD curves of the MSNMSeHS, and MSNMOHS at current density of  $2 \text{ A g}^{-1}$ . (c) Nyquist plots of the MSNMSeHS, and MSNMOHS electrodes.

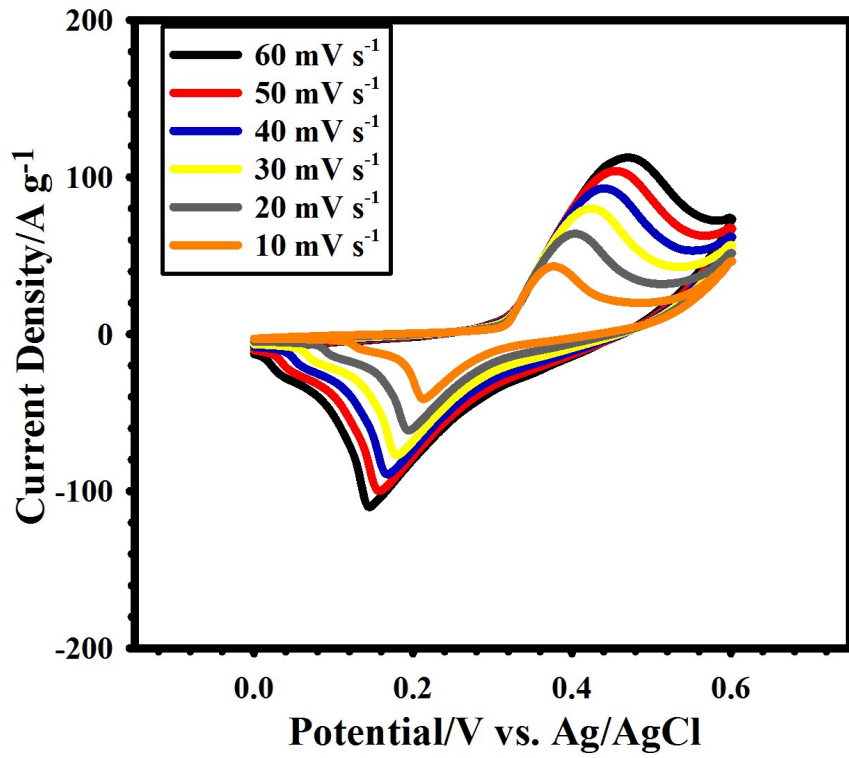


**Fig. S5.** CV graphs of the MSNMOHS electrode at various scan rates.

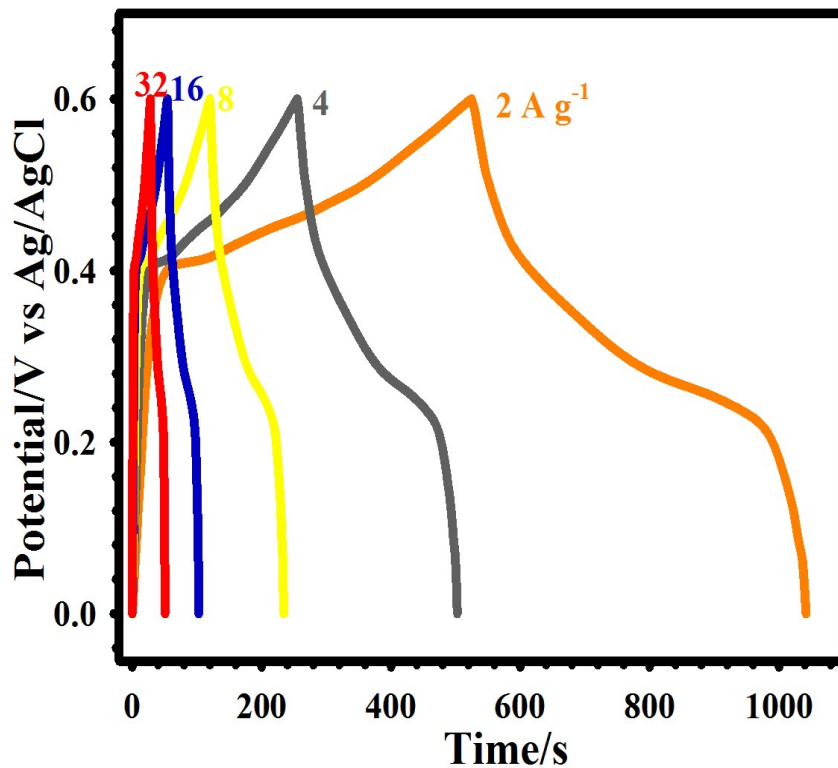


**Fig. S6.** GCD plots of the MSNMOHS electrode at various current densities.

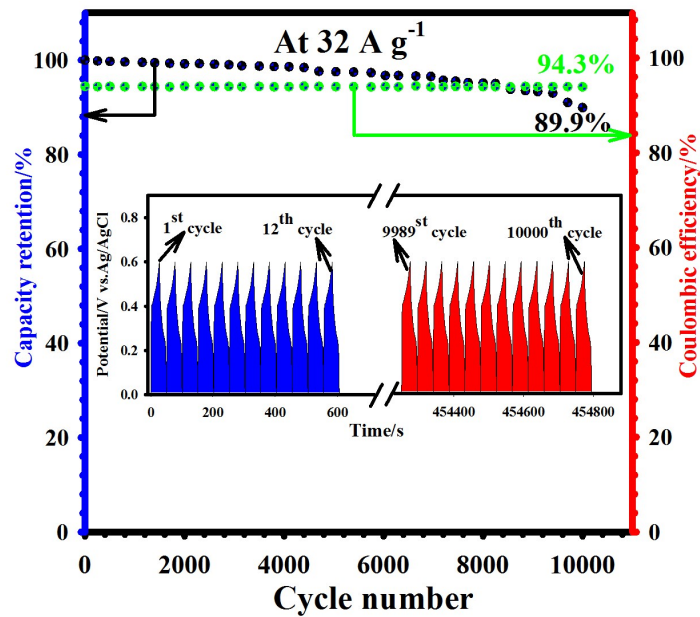


**Fig. S7.** Durability of the MSNMOHS electrode

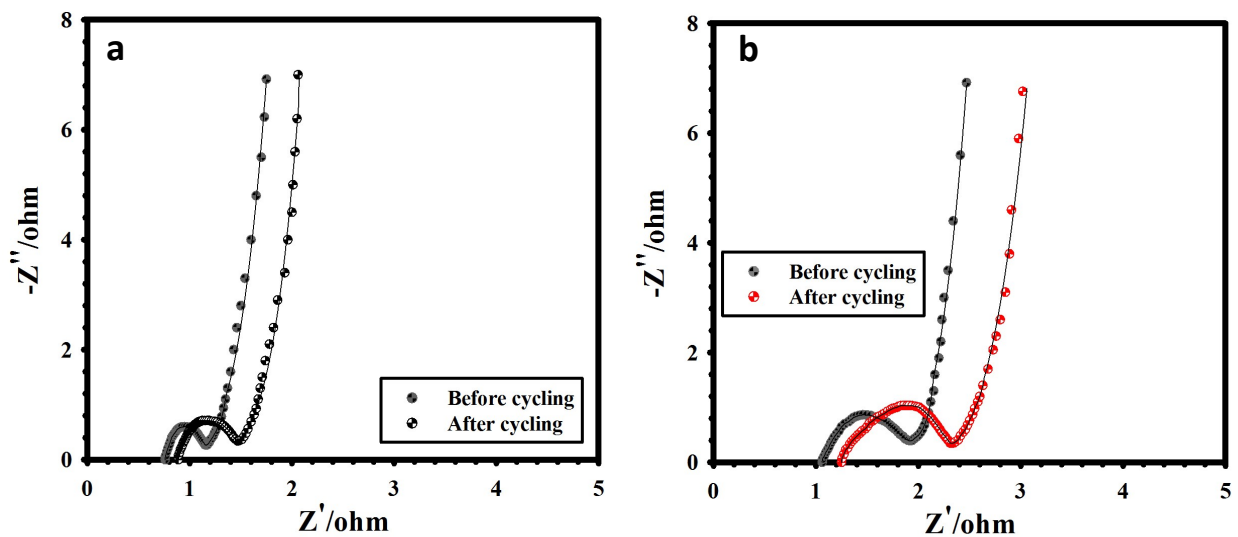


**Fig. S8.** (a) Nyquist graphs of the MSNMSeHS electrode before and after cycling. (b) Nyquist graphs of the MSNMOHS electrode before and after cycling.

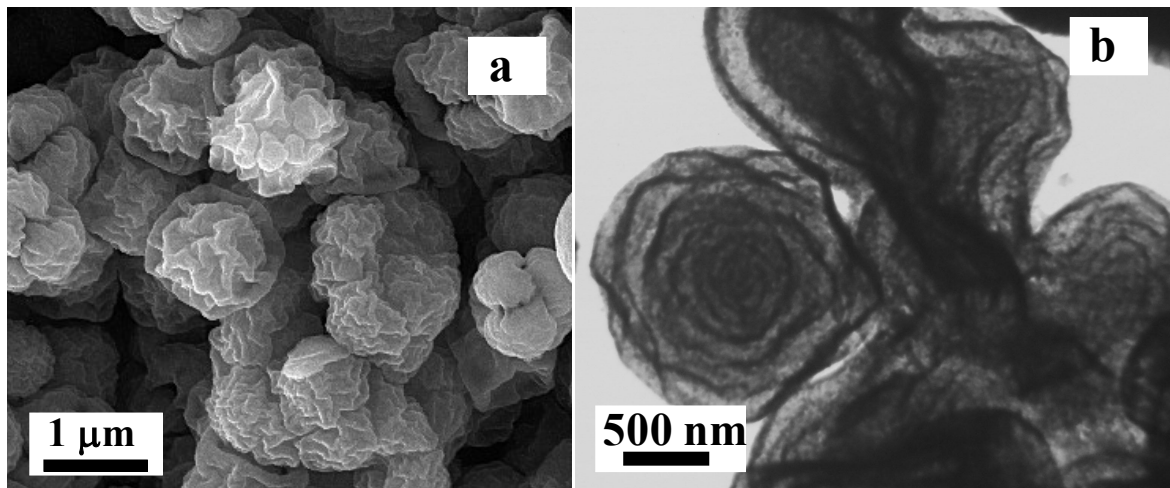


**Fig. S9.** (a) FE-SEM image of the MSNMSeHS after cycling. (b) TEM image of the MSNMSeHS after cycling.

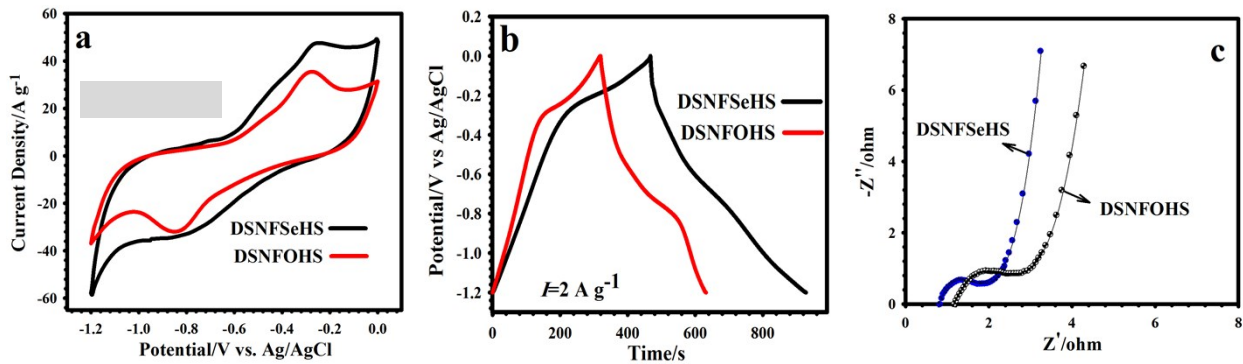


**Fig. S10.** (a) CV curves of the DSNFSeHS and DSNFOHS electrodes at scan rate of  $60 \text{ mV s}^{-1}$ . (b) GCD curves of the DSNFSeHS and DSNFOHS electrodes at current density of  $2 \text{ A g}^{-1}$ . (c) Nyquist plots of the DSNFSeHS and DSNFOHS electrodes.

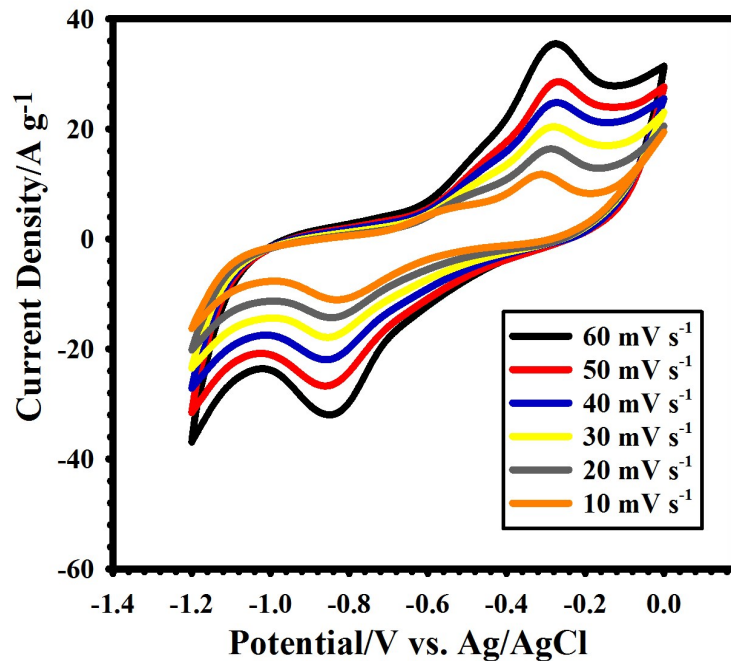


**Fig. S11.** CV curves of the DSNFOHS electrode at various scan rates

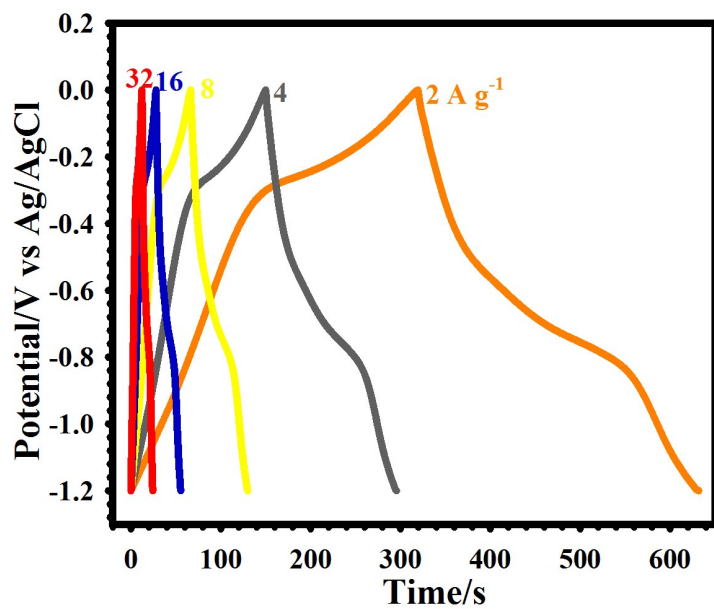


**Fig. S12.** GCD curves of the DSNFOHS electrode at various current densities.

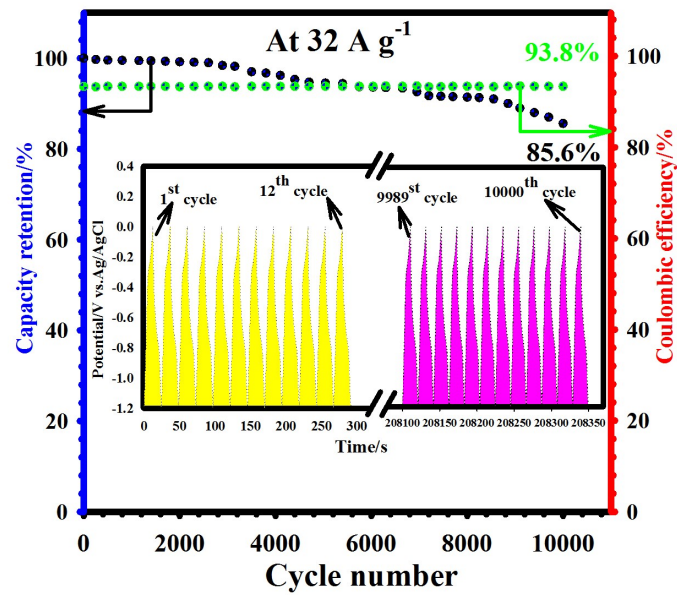


**Fig. S13.** Durability of the DSNFOHS electrode.

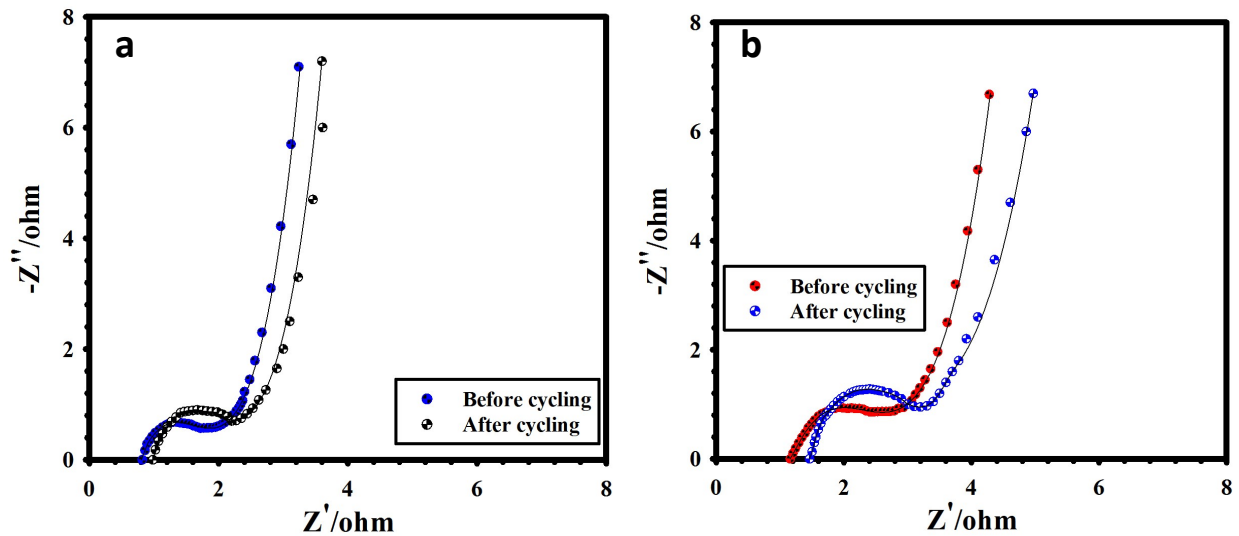


**Fig. S14.** (a) Nyquist graphs of the DSNFSeHS electrode before and after cycling. (b) Nyquist graphs of the DSNFOHS electrode before and after cycling.

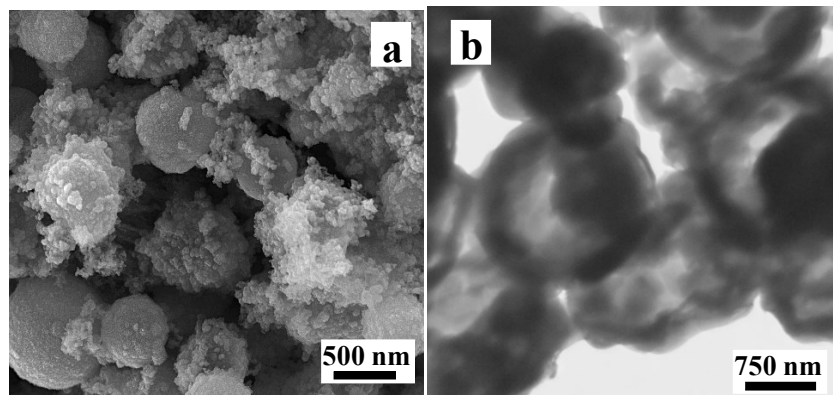


**Fig. S15.** (a) FE-SEM image of the DSNFSeHS after cycling. (b) TEM image of the DSNFSeHS after cycling.

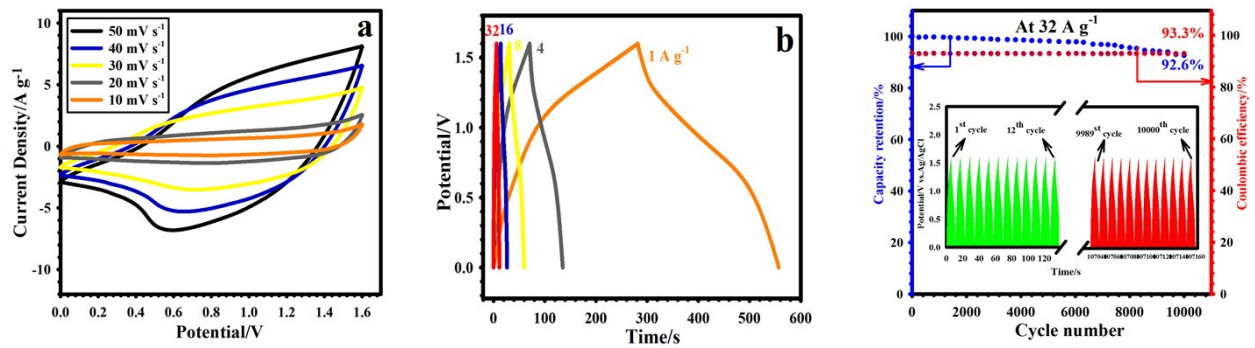


**Fig. S16.** (a) CV curves of the MSNMSeHS||AC at various scan rates. (b) GCD curves of the MSNMSeHS||AC at various current densities. (c) Durability of the MSNMSeHS||AC device.

**Table S1.** Comparison of the electrochemical performance of the MSNMSeHS cathode electrode in three and two electrode systems with other previously reported electrodes.

Composition	Capacity 3 and 2 electrodes (mAh/g or C/g)	Cycles, retention 2 and 3 electrode	Rate capability, 2 and 3 electrodes	ED (W h kg <sup>-1</sup> ) 2 Electrode	Reference
Ni <sub>0.67</sub> Co <sub>0.33</sub> Se <sub>2</sub>	447 C/g at 1 A/g (3 E)	2000, 97% (3 E) 5000, 83.3% (2 E)	56% at 50 A/g (3 E)	38.1	1
Ni <sub>0.6</sub> Co <sub>0.4</sub> Se <sub>2</sub>	602.6 C/g at 1 A/g (3 E)	5000, 91% (2 E)	77.7% at 20 A/g (3 E)	42.1	2
Ni <sub>0.85</sub> Se	114.6 mAh/g at 1 A/g (3 E)	5000, 73.9% (3 E) 5000, 76% (2 E)	60.5% at 10 A/g (3 E)	22.3	3
Ni <sub>1.5</sub> Co <sub>1.5</sub> S <sub>4</sub> @Ti <sub>3</sub> C <sub>2</sub> -5	166.7 mAh/g at 1 A/g (3 E)	3000, 78.7% (3 E) 8000, 90% (2 E)	73.9% at 20 A/g (3 E)	49.8	4
Copper cobalt selenide	562 C/g at 1 A/g(3 E)	5000, 94.5% (3 E)	73% at 60 A/g (3 E)	32.4	5
NiSe <sub>2</sub> /rGO	137.7 mAh/g at 1 A/g (3 E)	2500, 80.7% (3 E) 10000, 80% (2 E)	-	33.13	6
Co-Cd-Se	192 mAh/g at 1 A/g (3 E)	1000, 95.2% (3 E) 1000, 80.9% (2 E)	-	57.6	7
CoSe <sub>2</sub> /MoSe <sub>2</sub> -3-1	211.97 mAh/g at 1 A/g (3 E)	2000, 94.2% (3 E) 10000, 93.4% (2 E)	67.8% at 30 A/g (3 E)	51.84	8
MSNMSeHS	339.2 mAh/g/1221.1 C/g (3 E) 125.1 mAh/g/ 450.36 C/g at 1 A/g (2 E)	10000, 95.7 (3 E) 10000, 94.4 (2 E)	78.8% at 32 A/g (3 E)	112.6	This work

**Table S2.** Comparison of the electrochemical performance of the DSNFSeHS anode electrode in three electrode system with other previously reported electrodes.

Composition	Capacity 3 electrode (mAh g <sup>-1</sup> or C g <sup>-1</sup> )	Cycles, retention 3 electrode	Rate capability 3 electrodes	Reference	
Fe <sub>2</sub> O <sub>3</sub> @Fe <sub>3</sub> C@C	611 C g <sup>-1</sup> at 1 A g <sup>-1</sup> (3 E)	-	%68.41 at 10 A/g	9	
Fe <sub>2</sub> O <sub>3</sub> @NG/CFC	66.1 mAh/g at 2 A g <sup>-1</sup>	10000, 95.1%	69% at 50 A/g	10	
Fe <sub>2</sub> O <sub>3</sub>	81.9 mAh/g at 1 A g <sup>-1</sup>	5000, 84.2%	55.6% at 20 A/g	11	
P-FeS <sub>2</sub> /GNS	246 mAh/g at 3 A/g	5000, 93%	-	12	
FeS <sub>2</sub>	515 C/g at 1 A g <sup>-1</sup> (3 E)	-	65% at 20 A/g	13	
FeS <sub>2</sub> /GNS	793 C/g at 3 A g <sup>-1</sup>	-	82% at 30 A/g	14	
Fe <sub>2</sub> O <sub>3</sub> @NG	145.3 mAh/g at 1 A/g	10000, 89.5%	57.7% at 50 A/g	15	
Fe <sub>2</sub> O <sub>3</sub> /G	48 mAh/g at 0.5 A/g	5000, 92.5%	57.7% at 20 A/g	16	
DSNFSeHS	258.4 mAh/g/930.25 C/g	10000, 90.9%	75.5% at 32 A/g	This work	

## References

- Y. Hu, C. Huang, S. Jiang, Y. Qin and H. C. Chen, *J. Colloid Interface Sci.* 2020, **558**, 291–300.
- Y. Wang, R. Liu, S. Sun and X. Wu, *J. Colloid Interface Sci.* 2019, **549**, 16–21.
- S. Wu, Q. Hu, L. Wu, J. Li, H. Peng and Q. Yang, *J. Alloys Compd.* 2019, **784**, 347–353.

- 4 X. He, T. Bi, X. Zheng, W. Zhu and J. Jiang, *Electrochim. Acta* 2019, **322**, 134759.
- 5 S. E. Moosavifard, F. Saleki, A. Mohammadi, A. Hafizi and M. R. Rahimpour, *J. Electroanal. Chem.* 2020, **871**, 114295.
- 6 G. S. Wu, T. Cui, Q. Hu, F. Yin, Q. Feng, S. Zhou, Q. Su, L. Wu and Q. Yang, *Synth. Met.* 2020, **268**, 116490.
- 7 Z.-B. Zhai, K.-J. Huang and X. Wu, *Nano Energy*, 2018, **47**, 89-95.
- 8 F. Ma, J. Lu, L. Pu, W. Wang and Y. Dai, *J. Colloid Interface Sci.* 2020, **563**, 435-446.
- 9 S. Dai, Y. Bai, W. Shen, S. Zhang, H. Hu, J. Fu, X. Wang, C. Hu and M. Liu, *J. Power Sources* 2021, **482**, 228915.
- 10 T. T. Nguyen, J. Balamurugan, N. H. Kim and J. H. Lee, *J. Mater. Chem. A* 2018, **6**, 8669-8681.
- 11 J. Lin, Y. Yan, H. Wang, X. Zheng, Z. Jiang, Y. Wang, J. Qi, J. Cao, W. Fei and J. Feng, *J. Alloys Compd.* 2019, **794**, 255-260.
- 12 Z. Sun, F. Li, Z. Ma, Q. Wang and F. Qu, *J. Alloys Compd.* 2021, **854**, 157114.
- 13 Z. Sun, X. Yang, H. Lin, F. Zhang, Q. Wang and F. Qu *Inorg. Chem. Front.* 2019, **6**, 659-670.
- 14 Z. Sun, H. Lin, F. Zhang, X. Yang, H. Jiang, Q. Wang and F. Qu, *J. Mater. Chem. A* 2018, **6**, 14956-14966.
- 15 R. Balaji, J. Balamurugan, T. T. Nguyen, N. H. Kim and J. H. Lee, *Chem. Eng. J.* 2020, **390**, 124557.
- 16 P. Bandyopadhyay, G. Saeed, N. H. Kim and J. H. Lee, *Chem. Eng. J.* 2020, **384**, 123357.